

The Bio-inspired Design of a Self-propelling Robot Driven by Changes in Humidity

Raphael Kay¹, Kevin Nitiema², David Correa³

¹University of Toronto ²University of Toronto ³University of Waterloo

^{1,2}{raphael.kay|kevin.nitiema}@mail.utoronto.ca ³david.correa@uwaterloo.ca

Plants use highly reliable nastic movement through the oriented hygroscopic swelling of tissue to autonomously respond to external stimuli. Buildings, on the other hand, use highly unreliable kinematic mechanisms with multiple failure-prone components that are dependent on electromechanical input. Literature describing stimulus-responsive shape-changing actuators focuses primarily on single-stage reversible movements, and therefore provides limited insights into the methodologies needed to achieve directed multistage locomotion. Here we describe a methodology to develop a self-propelling and programmable robot (Hygrobot) capable of flexible locomotion with the cyclic introduction and removal of moisture. Several multi-layer mechanisms were programmed to actuate sequentially with changes in moisture, in a choreographed manner, to generate locomotion. We expect that this approach can advance interest into hygroscopic self-propelled mechanisms, as well as foster further research into the development of more complex kinematic mechanisms, requiring articulated and multi-stage actuation, for direct architectural or robotic implementation.

Keywords: *Bio-inspired, shape-changing, programmable materials, robotic locomotion*

INTRODUCTION

Wood is a hygroscopic material. With a change in moisture content, it shrinks and swells anisotropically, affecting strength, stiffness, and fracture morphology (Dinwoodie, 2000). Commonly regarded as a deficiency (Simpson, 1983), nature has found multiple avenues to augment and expand the dimensional change of cellulose tissue as a highly efficient actuation mechanism. Unlike plant movements actively driven by turgor variations and osmotic gradient, which require the plant to be alive and re-

quire metabolic energy, passive swelling and shrinking of tissue can occur long after the plant is dead - even in semi-fossilized structures (Poppinga et al., 2018; Poppinga, 2015). In other words, the direction and magnitude of actuation is programmed in the structure of the tissue itself and therefore operates autonomously in response to external signals like humidity. Passive swelling drives the movement of wheat awns, the self-burial of seeds, the shrinkage of some types of mosses, and the opening and closing of pinecone scales (Reyssat and Mahadevan,

2009). Pinecone scales are a key bio-mimetic model for bilayer material structures that curl in response to moisture. They open when the air is dry and close when the air is wet, a reversible and repeatable process vital for fertilization (Figure 1B-1C). This shape-change is passive, and is considered to be 'biologically programmed' within the tissue (Dawson et al., 1997).

Stress-induced bending in bilayers was established by Timoshenko in his work with bi-metal thermostats (Timoshenko, 1925). This functional bilayer principle has been widely referenced in the literature regarding stimulus responsive shape-changing mechanisms. This includes hygroscopic wood mechanisms (Reichert et al., 2015, Rugeberg and Burgert, 2015, Holstov et al., 2015), 4D printed mecha-

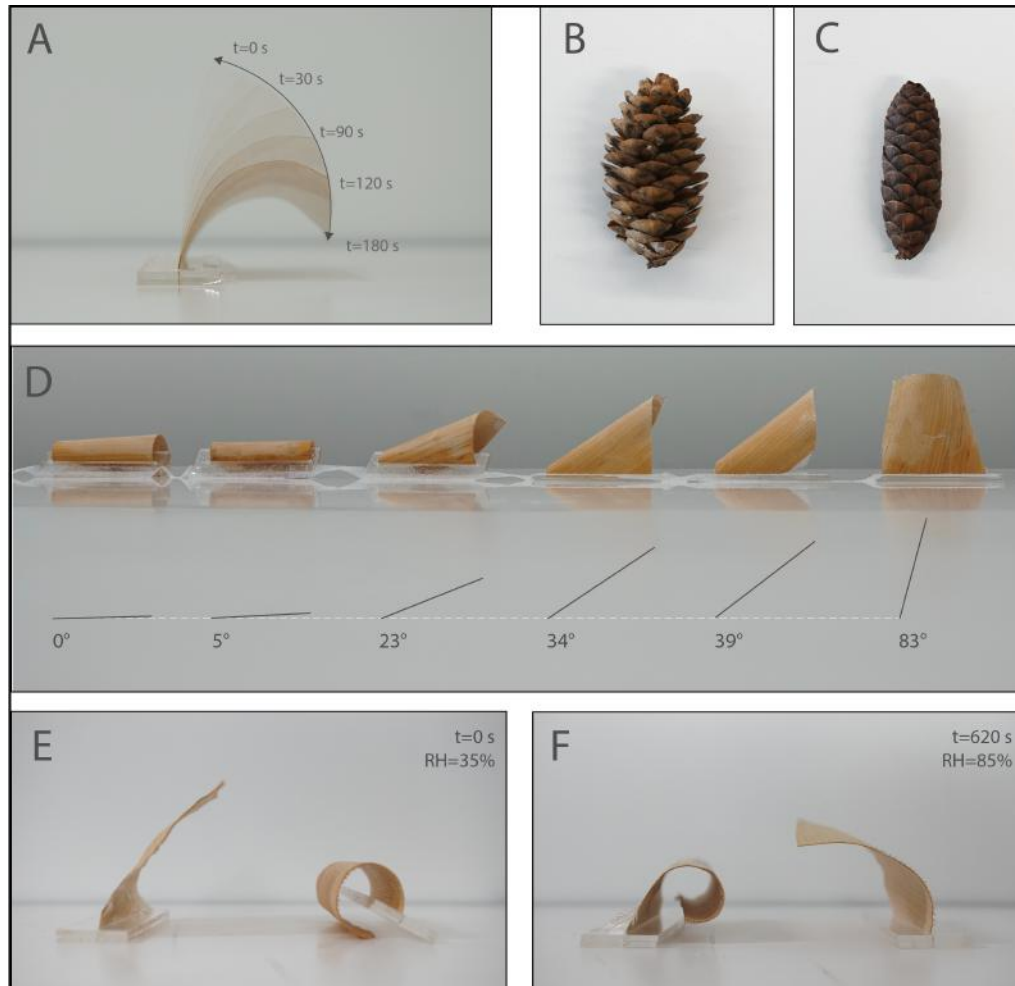


Figure 1
 A: Hygroscopic bend initiated by changing relative humidity in air over time in a wood veneer and fiberglass bilayer.
 B-C: Hygroscopic bend initiated by increasing relative humidity in air over time in a pinecone scale ($t=0$ and $RH=10\%$, to $t=25$ min and $RH=85\%$).
 D: Differences in bend angle depending on grain direction after moisture introduction ($t=180$ s, $RH=85\%$).
 E-F: Differences in bend direction depending on moisture level of active layer at fabrication (left sample in both E, F fabricated at $RH=35\%$ and right sample in both E, F fabricated at $RH=85\%$).

nisms (Tibbits, 2014, Wood et al., 2016, Gladman et al., 2016, Han et al., 2018), thermo-responsive metal bilayers (Sung, 2016), and hybrid wood-metal composites (Abdelmohsen et al., 2019). Samples are generally developed to achieve continuous curvature but localized bending has also been proposed by limiting the bilayer region relative to the sample, to form hinge like mechanisms (Tibbits, 2014).

Wood is a naturally grown material with a highly oriented structure that is highly differentiated based on the wood grain orientation (Gibson and Ashby, 1997). Hygroscopic expansion is highly variable between wood species or even within different specimens of the same tree due to natural variation (Dinwoodie, 2000). Moisture-responsive shape-changing bilayers have been fabricated by bonding quarter sawn maple with an inactive layer of glass fiber textile (Reichert et al., 2015, Holstov et al., 2015, Abdelmohsen et al., 2019), or by cross laminating maple or beech with spruce veneer (low hygroscopic swelling) to create an all-wood bilayer (Wood et al., 2016, Rugeberg and Burgert, 2015, Dierichs, 2017). Testing of glues and optimized fabrication parameters for wood bilayers has provided valuable insight into the large-scale implications that this system may offer (Vailati et al., 2017, Vailati et al., 2018). Beyond wood lamination, there has also been ongoing research into the potential of 3D printing in the development of wood polymer composite bilayers, using wood or cellulose fibers embedded in polymer inks (Gladman et al., 2016, Erb et al., 2013, Correa et al., 2015).

In architecture, Michelle Addington (2005) states that “Smart Materials are essentially material systems with embedded technological functions”. These functions, and specifically the computational capacity of materials, have fascinated engineers, physicists, and architects (Addington, 2005; Harding, Miller, and Rietman, 2008; Toffoli and Margolus, 1991). Using this “material intelligence” (Kwinter, 2001), in conjunction with the cyclical changes in humidity and temperature, these hygroscopic actuation mechanisms can have a key role in reducing energy consumption and carbon emissions in the built environ-

ment (Poppinga et al., 2018). Applications of hygroscopic wood actuators in architecture include building skins (Reichert et al., 2015), larger scale shading mechanisms (Vailati et al., 2017), and a solar tracking device for photovoltaic applications (Rugeberg and Burgert, 2015). However, all of these existing actuators are fixed in place, and at the moment there is limited literature that investigates their potential as untethered systems capable of moving independently. Research by Dierichs and Wood has addressed the potential of granular climate responsive components capable of re-configurable self-assembly (Dierichs, 2017), but no known research exists that has particularly looked at locomotion as the key performance driver for hygroscopic mechanisms. The presented paper accordingly outlines a proof of concept that demonstrates a primitive four-legged robot (Hygrobot) programmed to self-propel with a change in humidity. We demonstrate and quantify the potential for a localized bilayer region to limit the angle of curvature and produce a joint-like bending effect for multistage locomotion.

MATERIALS AND METHODS

System Variables

The stimulus-responsive behaviour of a hygroscopic bilayer system is affected by a series of parameters. These parameters can be controlled to calibrate when, and how, a bend will occur.

Active Layer Type and Thickness. Quarter-sawn maple veneer with 0.8 mm thickness was used as the active layer. Maple was selected given its lower modulus of elasticity, grain direction homogeneity, and decay resistance (Reichert et al., 2015). A quarter-sawn veneer cut was selected due to greater consistency in grain and radial expansion (Dinwoodie, 2000). Consistency in the grain direction is important as this directionality is directly correlated to the direction of swelling. Changing the angle of grain orientation in the sample correlates to a change in the direction of bending (Figure 1D).

The actuation response time is directly affected by the rate of moisture diffusion throughout the component. Therefore, larger thickness in the active layer requires more time to reach equilibrium, holding off natural deformation for longer (Reichert et al., 2015). The time required for the bilayer to shape-change is determined by the speed of change in the relative humidity and the rate of moisture intake by the sample.

Inactive Layer Type. The restrictive layer constrains the expansion of wood. Based on the referenced literature and preliminary testing, either an epoxy and fiberglass layer (Figure 1), or a strictly epoxy layer was used throughout this work.

Relative Humidity. Moisture is the primary driver of movement in hygroscopic bilayers, and specifically relative humidity (RH). RH represents the ratio of the vapour pressure of the air to the saturated vapour pressure of the air (Dinwoodie, 2000). For a given vapour pressure and air temperature, there is an equilibrium moisture content for wood where no vapour will travel in or out. As the vapour pressure or temperature changes, so too does the moisture content of the wood, attempting to reach equilibrium (Dinwoodie, 2000). When wood is bonded to an inactive layer, environmentally sealed on one side, a stress gradient occurs between the two layers, resulting in the bending of the bilayer. As such, we can define the behaviour of a hygroscopic bilayer bend in terms of the relative humidity of its surrounding air.

RH can also be defined as a function of the absolute moisture content in the air and the air temperature. Warm air can hold more water than cold air, meaning for a given amount of moisture in the air, as temperature increases, the % RH will decrease. Accordingly, % RH can be changed by adjusting the absolute moisture content in the air while leaving the temperature, or by adjusting the temperature while leaving the absolute moisture content (Dinwoodie, 2000). Because of the above relationship, changes in temperature can have a direct effect on % RH. As such, experiments were conducted in a sealed environmental chamber, or a room with a consistent air

temperature (approx. 23° C). To change humidity, a series of ultrasonic humidifiers were used throughout the research.

Moisture Content of Active Layer at Bond. The shape of the wood layer and moisture content at the time of lamination corresponds with its rest condition. A bilayer laminated at low moisture will bend upon moisture intake. Oppositely, a bilayer laminated at high moisture will bend during moisture desorption. Any bilayer can be programmed to bend at a specific humidity, depending on the moisture content of the wood at the time of lamination. Figure 1E-F shows a bilayer laminated at low moisture content and a bilayer laminated at high moisture content first in low RH and then in high RH. The addition of moisture into the air can be seen to have the opposite shape-change effect on each bilayer.

Preliminary Experiments

Grain orientation and moisture content of the active layer at bond were tested individually. For both experiments active samples (maple veneer) were laser cut to the same square shape, 10 cm x 10 cm in size. In the first experiment, samples were cut at a different angle relative to the grain, ranging from 0° to 83°. The samples were prepared in a low RH environment using a drying oven for 30 minutes at 100° C, and lamination and curing was conducted in low RH (approx. 10% RH at 23° C). The samples were exposed to a change from 35% RH to 85% RH, while the temperature was kept constant at 23° C (Figure 1D). In the second experiment, samples were bonded at either low (approx. 10% RH at 23° C) or high RH (approx. 70% RH at 23° C), and the effect of moisture introduction and removal was observed (Figure 1E-F).

Hinge Experiments

To study the effect of hinge location on bilayer sample bending, eight veneer samples were fabricated measuring 5 cm x 15 cm each. Samples were prepared in a low RH environment (approx. 10% RH at 23° C). Samples were fabricated with controlled local bilayer regions (as opposed to the full length of

the sample). Each region was created by pressing the maple veneer layer against a stamp of a controlled size, sealing the veneer samples within the region of contact only. The size of the contact region remained consistent throughout this experiment (15 mm x 5 cm), and the location was varied experimentally (Figure 3B-C). To study the effect of hinge size on bilayer sample bending, eight bilayer samples were fabricated in the same manner as above. In each case, the stamp thickness varied in size. The location of the contact region centre remained consistent, about 4 cm from the fastening axis (Figure 3D-E).

Hygrobot Fabrication

The Hygrobot uses four actuated legs attached to an inactive acrylic body. Each leg measures 8 cm long and 1.75 cm wide. The legs were prepared using the epoxy stamping methods described above, and stamps were applied halfway up each leg to create localized bending, mimicking the effect of a knee joint. The feet of the legs were given claws to increase friction during movement. The 0.75 mm thick acrylic body was hollowed out to reduce weight. The legs were attached to the body using fishing cord and two-part epoxy resin. Figure 4 (right) shows the Hygrobot at rest.

RESULTS

Preliminary Experiments

Individual tests were performed to demonstrate both the relationship between grain direction and moisture content of the active layer at bond to shape-change. This preliminary experimentation is consistent with previous literature (Reichert et al., 2015), demonstrating that the angle (Figure 1D) and direc-

tion (Figure 1E-F) of a bilayer bend can be controlled through the calibration of the material preparation and the fabrication process.

Computational Model

A geometric model was designed to approximate the curvature observed in physical samples when exposed to humidity (Figure 2). A linear relationship was then established between sample curvature and humidity and was used in this model to accurately predict bend severity between 35%-85% RH. The sample curvature change in bending was defined along a single arc, and was thus simplified to account only for uniaxial bending caused by the expansion or contraction of cellulose tissue in the active wood veneer component of the bilayer.

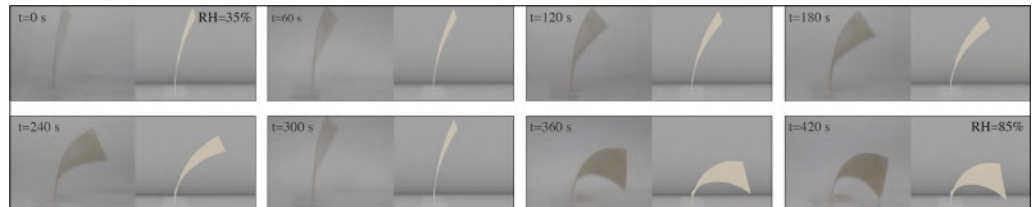
Location of Hinge

The relationship between the location of a targeted bilayer and the overall bend of a sample was tested. The bilayer location was changed relative to the fastening axis across eight samples, varying in distance (14 mm intervals), beginning at 3.5 mm from the axis (Figure 3B-3C). Equation 1 in Figure 3 shows the linear relationship between the seal location centre, x , in mm from the fastening axis, and percent aperture opening, $f(x)$, as viewed from the normal to the bilayer surface at C. The percent aperture opening is calculated by dividing the temporary aperture area (created with the bilayer bend) by the overall bilayer area at rest.

Size of Hinge

A subsequent experiment was conducted to test the relationship between the size of a targeted seal and the overall bend of a bilayer. The length of the local

Figure 2
Physical model (left)
against
computational
model (right) with a
change in humidity
and time



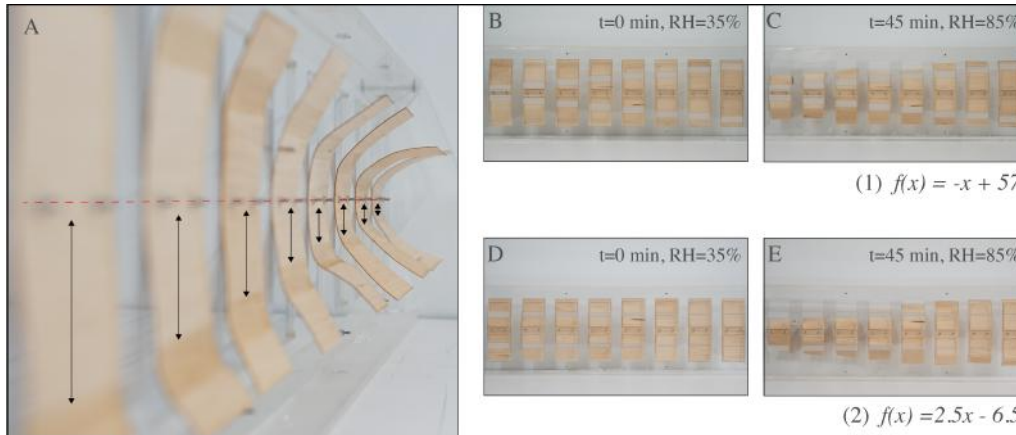


Figure 3
 A: The effect in the variation of targeted stamping location with moisture introduction on bend degree. Samples at $t=45$ min, $RH=85\%$. B-C: The effect in the variation of targeted stamping location with moisture introduction on bend degree. The grey rectangles represent the location of the stamp, and targeted bend axis. D-E: The effect in the variation of targeted stamping size with moisture introduction on bend degree. The grey rectangles represent the location of the stamp, and targeted bend axis.

targeted bilayer increased from 1 mm to 15 mm, increasing by intervals of 2 mm (Figure 3D-3E). Equation 2 in Figure 3 shows the linear relationship between the length of the seal, x , in mm, and the percent aperture opening, $f(x)$, as viewed from the normal to the bilayer surface at E. The percent aperture opening is calculated in the same manner as described above.

These tests demonstrate that a lamination methodology can be effectively used to control the degree of a bilayer bend. From this, we can program bilayer samples to achieve specific bending curvature in a reversible and repeatable manner.

Four Stage Movement of Hygrobot

Based on the presented control mechanisms, we developed a robot (Hygrobot) that could achieve independent locomotion, self-support, and self-propelled displacement across a given surface over time based on relative humidity changes in the environment. In nature, several biological organisms use friction to propel, or to amplify, their applied movement. For example, snakes rely on surface roughness to initiate their movement, and many other animals rely on obstacle or surface friction to climb or dig (Denny, 1980). Similarly, seeds use cellulose-based nastic motors to dig themselves into the ground

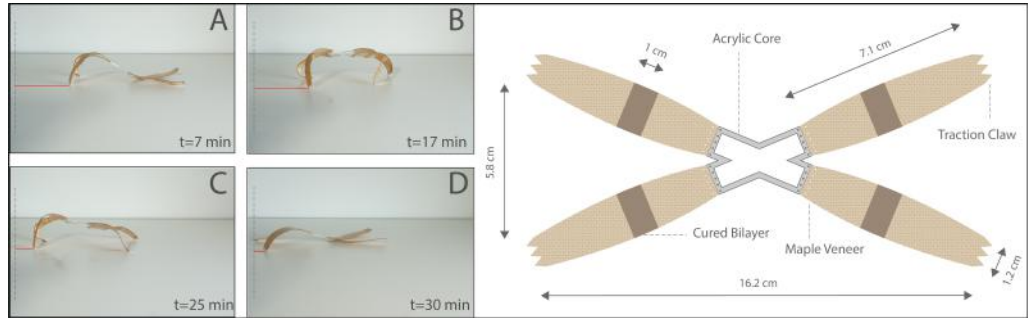
(Burgert and Fratzl, 2009). Existing literature presents various examples of abstract models that attempt to translate similar animal movement robotically (Shepherd et al., 2011). In our case, the movement of Hygrobot is based on a repeating set of four moves. Figure 4 displays each of these moves in order, illustrating cyclic motion.

The first step targets movement in the front legs, actuated through the local depositing of moisture via spray in an otherwise low-humidity environment. These legs were programmed to bend with high moisture (approx. 85% RH locally), such that when moisture is deposited, bending occurs at the bilayer joint. The moisture-induced bend causes the “locking” of the front legs to the ground, at which point, unable to overcome static friction, pull the back legs and body towards them (Figure 5A).

The second step targets movement in the back legs. Like the front legs, the back legs were programmed to bend with high moisture (approx. 85% RH locally), such that when moisture is deposited, bending occurs at the bilayer joint. The moisture-induced bend brings the back legs up towards the front legs (Figure 5B).

The third move involves further movement in the back legs. The back legs, which are currently bent, are actively dried using heat from a drier to flatten,

Figure 4
 Left: Four step cyclic movement of the robot with targeted humidity introduction and time. Right: Plan diagram of Hygrobot at rest (approx. 35% RH).



coming back to equilibrium moisture. This flattening motion pushes the robot forward, unlocking the front legs from the ground (Figure 5C).

In the fourth move the front legs return to equilibrium, flattening as they dry, and leaving the robot back in its rest state in a new position (Figure 5D).

The four-step cycle was repeated four times over the course of 127 minutes. Each cycle lasted roughly 30 minutes and the robot moved a total of 43 cm. The temperature and humidity in the room remained constant throughout the experiment ($T=24^{\circ}\text{C}$, $\text{RH}=35\%$) as moisture was introduced only locally to the legs. Figure 6 displays the progression of the Hygrobot over time.

DISCUSSION

We have fabricated a hygroscopic robot that can move with targeted moisture introduction and removal. This device is actuated using a four-step cycle, generated by locally depositing and removing moisture to the front and back legs in a coordinated sequence.

Limitations

The low thickness of the system's legs gives an adequately fast response to moisture changes in the air, but also proves to be a structural liability over time. Over-saturation can cause plastic deformation of the wood, rendering it non-elastic, and less responsive to humidity. Uneven moisture introduction

across the grain can also cause microstructural damage in the material, further reducing its responsiveness to humidity (Reichert et al., 2015). In almost all the sample experiments, noticeable differences in the responsiveness of the legs over time (> four cycles) were observed, and we speculate that the over-saturation from our experimental process was the cause. The time-scale for movement presents further challenges. The average speed of the Hygrobot through an entire cycle of movement is around 2.5 mm/min, far slower than many mechanized robotic systems.

Future Research

Hygrobot relies on targeted moisture introduction for locomotion. It is speculated that by programming the front and back legs to bend and dry at different moisture, a natural humidity cycle could drive locomotion entirely. For example, its back legs could be programmed to bend at a higher humidity than the front legs such that, with an increase in humidity to a fixed point, only the front legs would bend and, with a further increase in humidity to a second fixed point, the back legs would bend. Theoretically, if non-localized moisture cycles could be effectively demonstrated as drivers of movement, robots could be calibrated to move according to the outdoor, or indoor, humidity cycles in various locations, permitting predictable and repetitive moisture patterns.

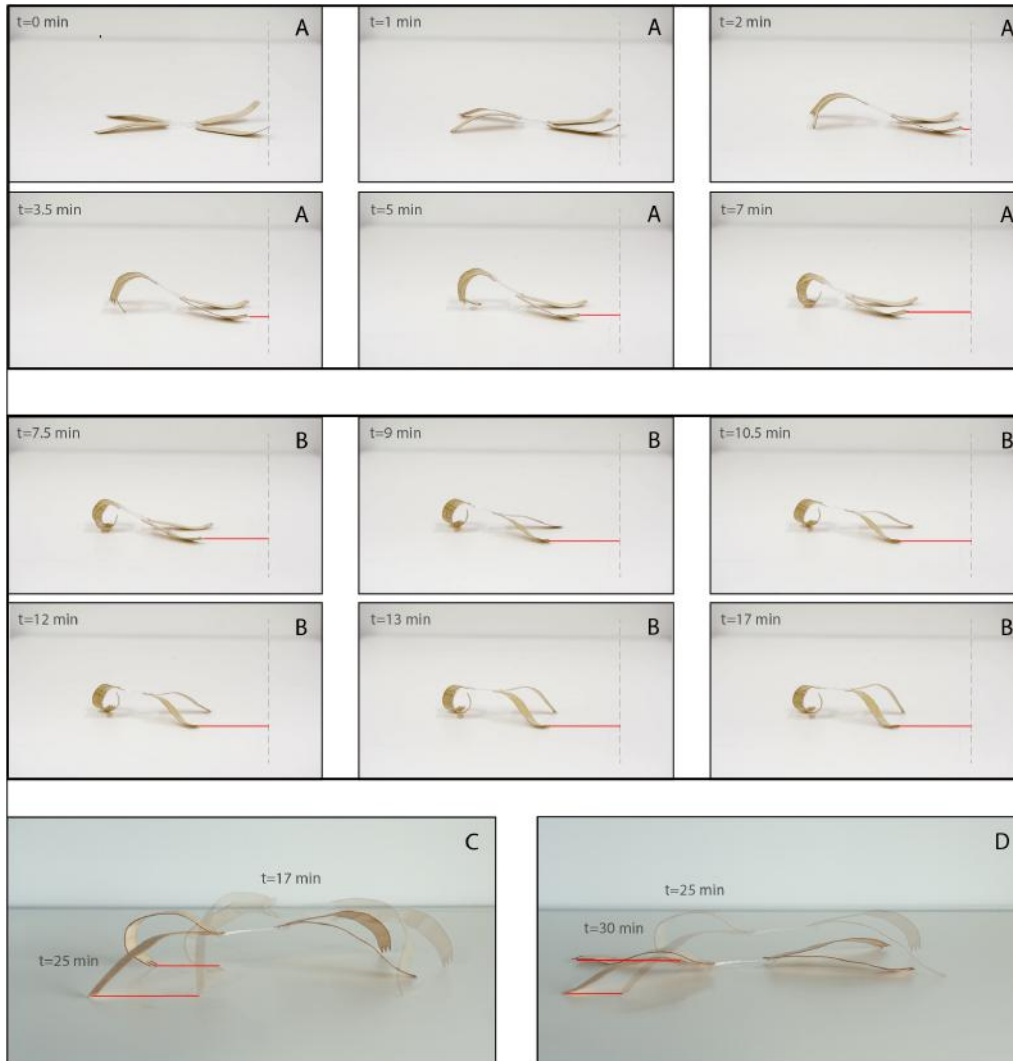
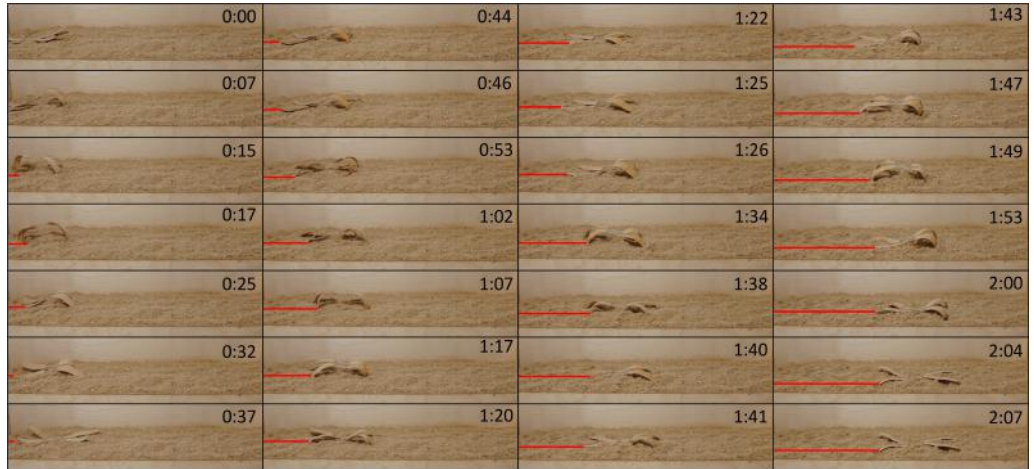


Figure 5
Locomotion of Hygrobot. A: The first move, with targeted movement of the front legs (left side of body). B: The second move, with targeted movement of the back legs (right side of body). C: The third move, with targeted movement of the back legs (right side of body). D: The fourth move, with passive drying releasing the body back to rest.

While moisture-induced movement due to daily fluctuations in arid regions would likely be dramatic but slow, tropical regions might allow for more rapid humidity fluctuations that could occur within a mat-

ter of hours. Future applications for locomotion remain speculative, but the ability to move through a landscape in search of specific environmental criteria, much like plant's seeds do, could provide valuable

Figure 6
Hyrgobot
progression over
time (in hours and
minutes). Final red
progress bar (2:07)
is 43 cm in length.



opportunities for terraforming. Furthermore, moisture induced changes in geometry could provide potential applications to reduce soil erosion and prevent landslides.

A variation in the curing process between right and left legs or in the angle of fastening relative to the grain could allow for turning capabilities, and thus multi-axis movement. Terrain conditions and feet geometry could also be further investigated.

Finally, there exists potential in expanding self-propelling robotic movement beyond hygroscopic systems. Similar mechanisms could be devised using temperature (thermal expansion in metal bilayers), or a combination of both active and passive systems as drivers and controllers of movement.

CONCLUSION

In this paper, we demonstrate a hygroscopically activated robot, capable of self-propelled locomotion and self-support with targeted moisture introduction and removal. Future studies should further investigate locomotion in direct relation to naturally occurring humidity cycles and with multi-directional flexibility.

Acknowledgements

RK and KN planned the research and performed all experiments with external guidance from DC. RK wrote the first draft of the manuscript. The consistent guidance of Nicholas Hoban was greatly appreciated throughout the project.

REFERENCES

- Abdelmohsen, S, Adriaenssens, S, El Dabaa, R, Gabriele, S, Olivieri, L and Teresi, L 2019, 'A multi-physics approach for modeling hygroscopic behavior in wood low-tech architectural adaptive systems', *Computer-Aided Design*, 106, pp. 43-53
- Addington, MD and Schodek, DL 2005, *Smart Materials and New Technologies: For the Architecture and Design Profession*, Elsevier, Amsterdam, London
- Burgert, I and Fratzl, P 2009, 'Actuation systems in plants as prototypes for bioinspired devices', *P. T. R. Soc.*, 367, pp. 1541-1557
- Correa, D, Papadopoulou, A, Guberan, C, Reichert, N, Menges, A and Tibbits, S 2015, '3D-Printed Wood: Programming Hygroscopic Material Transformation', *3D Printing and Additive Manufacturing*, 2, pp. 106-116
- Dawson, J, Vincent, JFV and Rocca, AM 1997, 'How pine cones open', *Nature*, 390, p. 668
- Denny, M 1980, 'Locomotion: the cost of gastropod crawling', *Science*, 208, pp. 1288-1290

- Dierichs, KW, Correa, D and Menges, A 2017 'Smart Granular Materials: Prototypes for Hygroscopically Actuated Shape-Changing Particles', *Proceedings of ACADIA 2017*, pp. 222-231
- Dinwoodie, JM 2000, *Timber, its nature and behaviour*, E & EF Spon, London
- Erb, RM, Sander, JS, Grisch, R and Studart, AR 2013, 'Self-shaping composites with programmable bio-inspired microstructures', *Nature Communications*, 4, p. 1712
- Gibson, LJ and Ashby, MF 1997, *Cellular solids: structure and properties*, Cambridge University Press
- Gladman, AS, Matsumoto, EA, Nuzzo, RG, Mahadevan, L and Lewis, JA 2016, 'Biomimetic 4D printing', *Nature Materials*, 15, p. 413
- Han, D, Lu, Z, Chester, SA and Lee, H 2018, 'Micro 3D Printing of a Temperature-Responsive Hydrogel Using Projection Micro-Stereolithography', *Scientific Reports*, 8, pp. 1-10
- Harding, S, Miller, JF and Reitman, EA 2008, 'Evolution in Materio: Exploiting the Physics of Materials for Computation', *Int J of Unconventional Computing*, 4(2), pp. 1-20
- Holstov, A, Bridgens, B and Farmer, G 2015, 'Hygromorphic materials for sustainable responsive architecture', *Construction and Building Materials*, 98, pp. 570-582
- Kwinter, S 2001, 'Physical Theory and Modernity: Einstein, Boccioni, Sant'elia', in Kwinter, S (eds) 2001, *Architectures of Time: Toward a Theory of the Event in Modernist Culture*, The MIT Press, Cambridge, MA, pp. 52-101
- Poppinga, S, Nestle, N, Sandor, A, Reible, B, Masselter, T, Bruchmann, B and Speck, T 2017, 'Hygroscopic motions of fossil conifer cones', *Scientific Reports*, 7, pp. 1-4
- Poppinga, S and Speck, T 2015 'New Insights into the Passive Nastic Motions of Pine Cone Scales and False Indusia in Ferns', *Plant Biomechanics International Conference 8*, pp. 202-207
- Poppinga, S, Zollfrank, C, Prucker, O, Ruhe, J, Menges, A, Cheng, T and Speck, T 2018, 'Toward a New Generation of Smart Biomimetic Actuators for Architecture', *Advanced Materials*, 30(19), pp. 1-10
- Reichert, S, Menges, A and Correa, D 2015, 'Meteorosensitive architecture: Biomimetic building skins based on materially embedded and hygroscopically enabled responsiveness', *Computer-Aided Design*, 60, pp. 50-69
- Reyssat, E and Mahadevan, L 2009, 'Hygromorphs: from pine cones to biomimetic bilayers', *J.R. Soc. Interface*, 6, pp. 951-957
- Ruggeberg, M and Burgert, I 2015, 'Bio-Inspired Wooden Actuators for Large Scale Applications', *PLoS One*, 10, pp. 1-16
- Shepherd, RF, Ilievski, F, Choi, W, Morin, SA, Stokes, AA, Mazzeo, AD, Chen, X, Wang, M and Whitesides, GM 2011, 'Multigait soft robot', *PNAS*, 108, pp. 20400-20403
- Simpson, WT 1983, 'Drying wood: a review', *Drying Technology*, 2, pp. 235-264
- Sung, D 2016, 'Smart geometries for smart materials: taming thermobimetals to behave', *J. Architectural Education*, 70, pp. 96-106
- Tibbits, S 2014, '4d Printing: Multi-Material Shape Change', *Architectural Design*, 84, pp. 116-121
- Timoshenko, S 1925, 'Analysis of bi-metal thermostats', *J. Optical Society of America*, 11, pp. 233-255
- Toffoli, T and Margolus, N 1991, 'Programmable Matter: Concepts and Realization', *Physica D: Nonlinear Phenomena*, 47(1-2), pp. 263-272
- Vailati, C, Hass, P, Burgert, I and Ruggeberg, M 2017, 'Upscaling of wood bilayers: design principles for controlling shape change and increasing moisture change rate', *Materials and Structures*, 50, pp. 1-12
- Vailati, C, Ruggeberg, M, Burgert, I and Hass, P 2018, 'The kinetics of wooden bilayers is not affected by different wood adhesive systems', *Wood Science and Technology*, 52, pp. 1589-1606
- Wood, DM, Correa, D, Krieg, OD and Menges, A 2016, 'Material computation - 4D timber construction: Towards building-scale hygroscopic actuated, self-constructing timber surfaces', *Int. J. Architectural Computing*, 14, pp. 49-62